Society for Immunotherapy of Cancer
Annual Meeting, November 2020
Abstract 583

Novel, Potent, and Selective Inhibitors of Hypoxia-Inducible Factor (HIF)-2α Reverse Pro-tumorigenic Transcriptional Programming in Cancer, Stromal, and Immune Cells

Dana Piovesan, Kenneth V. Lawson, Sean Cho, Akshata Udyavar, Jean Chan, Ada Chen, Jennie Au, Cesar Meleza, Xiaoning Zhao, Anh T. Tran, Samuel L. Drew, Balint Gal, Brandon R. Rosen, Manmohan Leleti, Elaine Ginn, Lixia Jin, Stephen W. Young, Jay P. Powers, Matthew J. Walters, Kelsey E. Sivick Gauthier

Arcus Biosciences, Inc.; 3928 Point Eden Way, Hayward, CA 94545 (USA)

OVERVIEW

- The solid tumor microenvironment (TME) can be hypoxic and cancer cells require induction of genes associated with metabolism, proliferation, and angiogenesis to survive and metastasize[1].
- The master transcriptional regulator of hypoxia-induced genes is the Hypoxia-Inducible Factor (HIF)[2]. HIF consists of an oxygen-regulated alpha monomer (of which there are three isoforms: HIF-1α, HIF-2α, and HIF-3α) that heterodimerize with a constitutively-expressed beta monomer (HIF-1β/ARNT)[2] (**Figure 1**).
- Allosteric disruption of HIF-α/HIF-1β heterodimer formation is an effective means to inhibit HIF-dependent gene transcription[2], and preclinical and clinical evidence suggests that inhibiting HIF-2α is a valid approach to block cancer progression, particularly in VHL disease-related cancers and clear cell renal carcinoma (ccRCC)[3,4,5].
- Here we describe pharmacological properties associated with a novel, potent, and selective advanced prototype HIF-2α inhibitor. We also highlight findings related to the understanding of HIF-2α biology in a model of tumor-associated macrophages (TAMs) as well as the development and application of HIF-2α-specific transcriptional signatures.

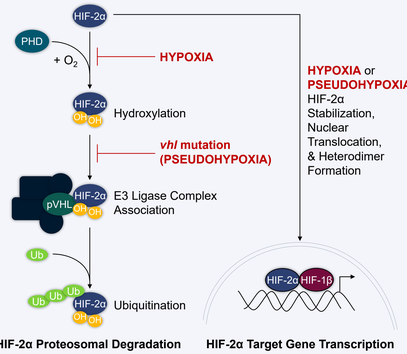

Figure 1. In normoxia, proline residues present in HIF-2α are hydroxylated by prolyl hydroxylases (PHDs), allowing for recognition by the von Hippel-Lindau (pVHL) E3-ubiquitin ligase complex, ubiquitination, and proteasomal degradation. Upon exposure to low oxygen conditions (hypoxia) or in the case of *vhl* mutation or silencing (pseudohypoxia), HIF-2α subunits accumulate, undergo nuclear translocation, and dimerize with HIF-1β/ARNT, resulting in transcription of pro-tumorigenic gene sets. Adapted from[6].

SUMMARY

- Optimized Arcus inhibitors, such as Compound 3, potently bind to and selectively inhibit HIF-2α, as demonstrated in biochemical, reporter, cancer cell line, and primary cell assays (**Figures 2-4, 6**).
- When orally administered to mice, Compound 3 was able to significantly decrease human tumor-derived HIF-2α-specific transcripts (**Figure 5**).
- HIF-2α inhibition reverses pro-tumorigenic gene expression and chemokine secretion by suppressive M2-polarized macrophages (an *in vitro* TAM model) while sparing CD8⁺ T cell functionality (**Figures 6 & 7**).
- Global transcriptomic analyses in M2 macrophages and a panel of cancer cell lines revealed minimal overlap between HIF-2α-specific gene signatures. Moreover, each cell type exhibited vastly different dependences upon HIF-2α for its respective hypoxic response (**Figure 8**).
- Interrogating clinical datasets with a broadly applicable "TAM" HIF-2α signature revealed indications that may benefit from combination of a HIF-2α inhibitor with etrumadenant (AB928) or AB680, Arcus molecules that block immunosuppressive adenosine signaling (**Figure 8**).
- Our novel HIF-2α inhibitor is expected to enter clinical trials in 2021.

RESULTS

Novel HIF-2α Inhibitor Compound 3 Potently Binds As Well As Inhibits HIF-2α-Mediated Transcription and Growth of Clear Cell Renal Cell Carcinoma Cells

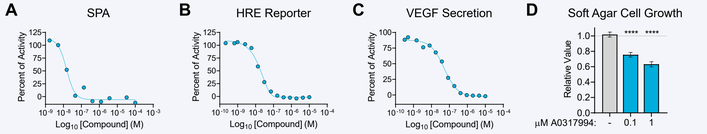

Figure 2. **Representative SAR assay examples for Compound 3. (A) Scintillation Proximity Assay (SPA).** Compound 3 binding to HIF-2α PAS-B domain was detected by displacement of ³H-tracer binding in SPA assay. **(B) Hypoxia-Responsive Element (HRE)-Luciferase Reporter.** Human 786-O renal adenocarcinoma cells (mutant *vhl* and *hif1a*) stably expressing HRE-luciferase reporter construct were treated with compound for 24 hrs prior to luciferase measurement. **(C) VEGF Secretion.** Secreted VEGF from 786-O cell culture medium after 24 hours compound treatment were detected using VEGF AlphaLISA (PerkinElmer). **(D) Soft Agar Cell Growth.** 786-O cells were embedded in 0.4% agar under a layer of media ± compound. Relative cell numbers were quantified after 8 days.****p<0.0001, Dunnett's multiple comparisons vs DMSO. Bars denote mean ± SEM.

Compound	HIF-2α SPA IC_{50} (nM ± SD)	786-O HRE Reporter IC_{50} (nM ± SD)	786-O Control Reporter IC_{50} (nM ± SD)	786-O VEGF Secretion IC_{50} (nM ± SD)
Compound 3	14.3 ± 2.0 (n=5)	14.0 ± 4.6 (n=9)	>10,000 (n=2)	44.1 ± 7.0 (n=2)
MK-6482 (PT2977, *competitor*)	22.4 ± 6.3 (n=3)	20.0 ± 1.1 (n=5)	>10,000 (n=6)	66.7 ± 26.4 (n=2)

Table 1. **Tabulated data for Arcus HIF-2α inhibitor Compound 3 and competitor compound MK-6482 (PT2977).** MK-6482 was synthesized utilizing published methodology[7].

Compound 3 Reverses HIF-2α-Driven Pro-angiogenic Programming in HUVEC Endothelial Cells

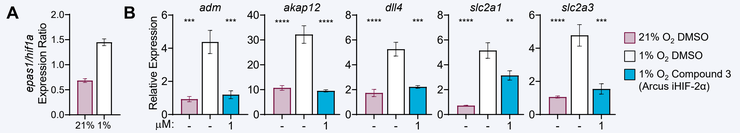

Figure 3. **(A) HUVEC HIF-2α/HIF-1α gene expression ratio increases in 1% O_2.** Shown is the *epas1:hif1a* gene expression ratio for HUVECs in 21% or 1% O_2. **(B)** HUVECs were treated with 1 μM Compound 3 in 21% or 1% O_2 and relative quantity ($2^{-\Delta Ct}$) of transcripts associated with angiogenesis. ****p<0.0001, ***p<0.001, **p<0.01, Dunnett's multiple comparisons vs 1% O_2 DMSO. Bars denote mean ± SEM.

Compound 3 Selectively Inhibits HIF-2α, and Not HIF-1α, Mediated Transcription

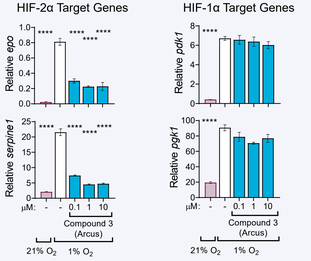

Figure 4. Hep3B hepatocellular carcinoma cells (wild-type *vhl* and *hif1a*) were exposed to normoxia (21% O_2) or hypoxia (1% O_2) and treated with 0.1, 1.0, or 10 μM of Arcus HIF-2α inhibitor Compound 3 in 1% O_2. Shown is the relative quantity ($2^{-\Delta Ct}$) of HIF-2α- (*epo* and *serpine1*) and HIF-1α- (*pdk1* and *pgk1*) specific transcripts. ****p<0.0001, ***p<0.001, **p<0.01, *p<0.05, Dunnett's multiple comparisons vs 1% O_2 DMSO (-). Bars denote mean ± SEM.

Compound 3 Inhibits HIF-2α-Specific Gene Targets in 786-O Xenograft Tumor-Bearing Mice

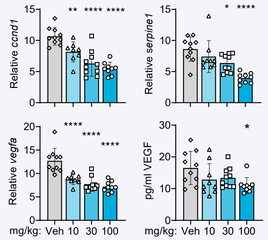

Figure 5. 786-O tumor-bearing mice received one dose of the indicated concentrations of Compound 3 and were assessed for tissue and plasma pharmacodynamic markers 24 hours later. Shown is the relative quantity of *ccnd1*, *serpine1* and *vegfa* in the tumor as well as VEGF protein levels in the serum. A preliminary human PK profile based on allometric scaling predicts that A0137994 is suitable for once daily oral dosing (data not shown). ****p<0.0001, ***p<0.001, **p<0.01, *p<0.05, Dunnett's multiple comparisons test vs Vehicle (Veh). Bars denote mean ± SD while symbols represent individuals.

RESULTS

Hypoxia Promotes a Pro-tumorigenic Macrophage Phenotype That is Markedly Reversed By HIF-2α Inhibition

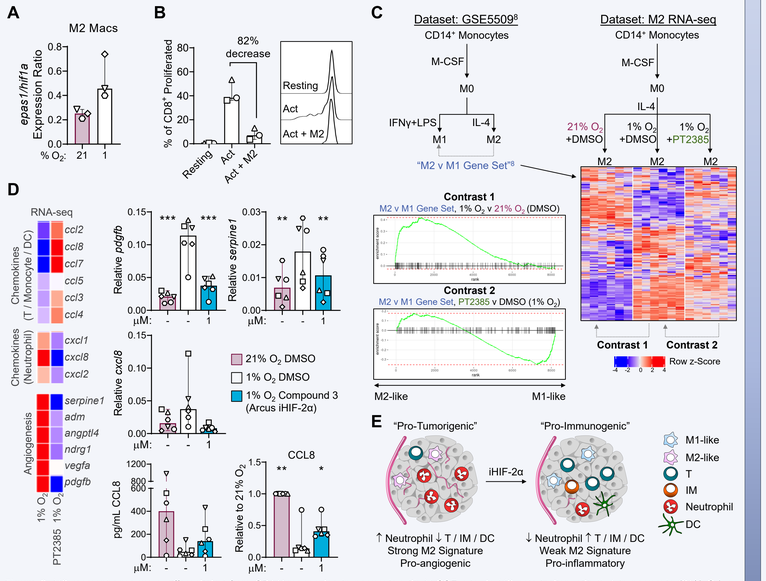

Figure 6. M0 macrophages were differentiated from CD14⁺ monocytes in normoxia with M-CSF prior to M2 polarization with IL-4 in normoxia (21% O_2) or hypoxia (1% O_2) with or without HIF-1α-HIF-2α inhibitor as indicated. **(A) M2 HIF-2α/HIF-1α gene expression ratio increases in 1% O_2.** Shown is the *epas1:hif1a* gene expression ratio for M2s in 21% or 1% O_2. **(B) M2s suppress CD8⁺ T cell proliferation.** CD8⁺ T cells ± Act were cultured alone or with autologous M2s in 1% O_2. Shown are the percent proliferation and proliferative peaks. **(C) M2-specific genes are upregulated in 1% O_2 and partially reversed by HIF-2α inhibition.** An M2-specific gene signature ("M2 versus (v) M1 Gene Set") derived from a publicly-available microarray dataset (LEFT, GSE5509[8]) was used to interrogate an experimentally-derived M2 RNA-seq dataset (RIGHT). Shown is a heat map depicting relative expression of the M2 v M1 Gene Set in the different conditions and GSEA plots depicting global changes in the M2 v M1 Gene Set in response to 1% O_2 and HIF-2α inhibition. Each heat map column is a unique donor. **(D) Transcript and secreted protein changes induced in 1% O_2 are reversed by HIF-2α inhibition in M2s.** M2s were treated with either 10 μM PT2385 or 1 μM Compound 3 (Arcus) in 1% O_2. Shown is a heat map (six donors averaged) of select chemokine and angiogenesis genes in 1% O_2 (vs 21% O_2) and with PT2385 in 1% O_2 (vs 1% O_2) and the relative quantity ($2^{-\Delta Ct}$) or pg/mL (raw and normalized) of indicated HIF-2α targets. ***p<0.001, **p<0.01 *p<0.05, Dunnett's multiple comparisons vs 1% O_2. **(E) Model: HIF-2α inhibition can reshape the TME through modulation of the pro-tumorigenic TAM M2 phenotype.** IM, Inflammatory monocyte; DC, Dendritic cell. For (A-C and E), symbols indicate donors and bars denote median ± range. PT2385 was synthesized utilizing published methodology[9].

HIF-2α Inhibition Does Not Impact CD8⁺ T Cell Functionality

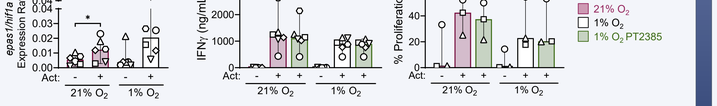

Figure 7. **(A) CD8⁺ T cell HIF-2α/HIF-1α gene expression ratio increases in 1% O_2.** Shown is the *epas1:hif1a* gene expression ratio for human CD8⁺ T cells ± TCR-mediated activation (Act) in 21% or 1% O_2. *p<0.05, Wilcoxon matched-pairs signed rank. **(B)** CD8⁺ T cells ± Act in 21% O_2 or 1% O_2 were treated with 10 μM of PT2385. Shown is secreted IFNγ and proliferation. ***p<0.001, **p<0.01, Dunnett's multiple comparisons vs respective - (DMSO) groups.

RESULTS

Application of Novel HIF-2α Gene Signatures Provides Rationale for Co-Targeting the HIF-2α and Adenosine Axes

Cell Line	Tissue	*vhl*
Hep3B	Hepatic	Wild Type
SW480	Colorectal	Wild Type
HCT116	Colorectal	Wild Type
MIA PaCa-2	Pancreatic	Wild Type
Panc-1	Pancreatic	Wild Type

Table 2. **Cancer cell lines used in HIF-2α signature development.**

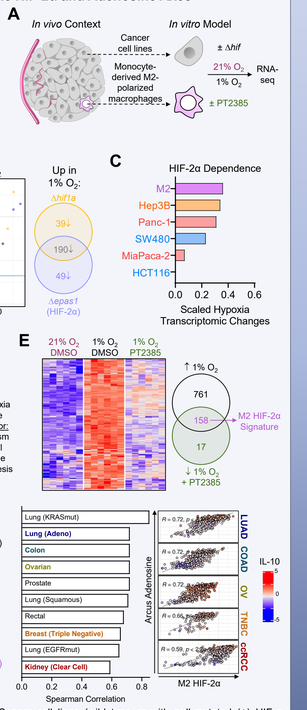

Figure 8. **(A) Experimental design.** Cancer cell lines (wild type or with null-mutated (Δ) HIF-α isoforms) and human *in vitro* polarized M2 macrophages in the presence or absence of PT2385 were exposed to 21% or 1% O_2 prior to RNA-seq. **(B) HIF-2α-specific genes were assigned by interrogating changes in ΔHIF-α or PT2385-treated conditions.** Shown is a volcano plot and Venn diagram depicting assignment of hypoxia-induced HIF isoform-specific genes in the Hep3B dataset. **(C) HIF-2α dependence is variable.** Hypoxia-dependent transcriptomic changes for each dataset were scaled (0-1). Shown is the relative contribution of HIF-2α to the global hypoxia response for each cell type. **(D) 1% O_2 induces a cancer cell line core hypoxia signature.** Shown is a Venn diagram of five cancer cell lines depicting the number of unique and common hypoxia-induced genes. **(E) M2s have a HIF-2α-induced gene signature that may be more broadly applicable than cancer cell-specific signatures.** Shown is a heat map and Venn diagram depicting 158 genes that are upregulated in 1% O_2 and significantly reversed by HIF-2α inhibition with PT2385. Each heat map column is a unique donor. **(F) Signature analyses in TCGA[12] revealed correlations between hypoxia, HIF-2α, & adenosine biology in ccRCC and beyond.** Shown is the correlation between various hypoxia signatures and a monocyte-derived dendritic cell (mo-DC) adenosine signature[11] derived by Arcus across TCGA and correlations between the M2 HIF-2α and the mo-DC adenosine signature in select indications.

1) Hockel (2001) 10.1093/jnci/93.4.266
2) Li (2019) 10.1021/acs.jmedchem.9b01596
3) Wallace (2016) 10.1158/0008-5472.CAN-16-0473
4) Chouiari (2020) 10.1200/jco.2020.38.6_suppl.611
5) Srinivasan (2020) 10.1200/jco.2020.38.15_suppl.5003
6) Yu (2019) 10.1016/j.drudis.2019.09.008
7) Xu (2019) 10.1021/acs.jmedchem.9b00719
8) Martinez (2006) 10.4049/jimmunol.177.10.7303
9) Wehn (2018) 10.1021/acs.jmedchem.8b01196
10) Liberzon (2015) 10.1016/j.cels.2015.12.004
11) DiRenzo (2019) 10.1186/s40425-019-0764-0
12) The results shown here are in part based upon data generated by the TCGA Research Network: https://www.cancer.gov/tcga